ACS Photonics

Article

pubs.acs.org/journal/apchd5

Nonmonotonic Wavelength-Dependent Power Scaling in Silicon-on-Insulator Waveguides via Nonlinear Optical Effect Conglomeration

Shawn Sederberg† and Abdulhakem Y. Elezzabi*

Ultrafast Optics and Nanophotonics Research Laboratory, University of Alberta, Edmonton, Alberta T6G 2 V4, Canada

Supporting Information

ABSTRACT: We experimentally investigate self-phase modulation (SPM) in silicon-on-insulator waveguides and present insight into the interplay between SPM and other nonlinear optical effects. Nonlinear interactions are studied in waveguides with cross-sectional widths in the range 260 nm $\leq w \leq$ 4150 nm, allowing for detailed study of the influence of mode confinement on SPM. It is found that both the mode confinement and peak intensity in the silicon waveguide are key in defining the nonlinear interaction. Power-scaling trends in different spectral ranges are presented, demonstrating the potential for multiple wavelength nonlinear functionalities in a single device.

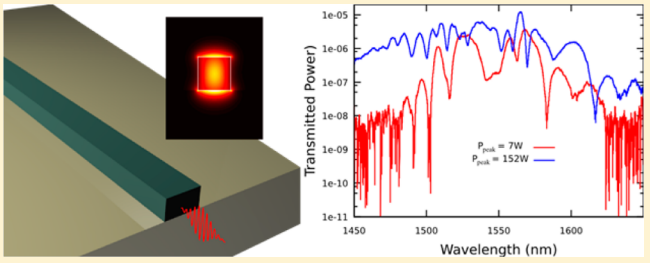

KEYWORDS: *waveguide, nonlinear optics, integrated photonics, ultrafast optics*

High-confinement silicon-on-insulator (SOI) waveguides offer attractive features that enable strong $\chi^{(3)}$ nonlinear interactions to accumulate when telecommunications band (1260 nm $\leq \lambda \leq$ 1675 nm) femtosecond pulses propagate through them.[1] For example, low linear losses in silicon (Si) at telecommunication wavelengths enable long nonlinear interaction lengths that are limited mainly by nonlinear losses (two-photon absorption (TPA) and free-carrier absorption (FCA)) and waveguide dispersion. Furthermore, Si has a high nonlinear coefficient[2] ($\chi^{(3)} = 2.97 \times 10^{15}$ cm^2/W), permitting strong nonlinear interactions to accumulate over much shorter lengths than other common waveguides.[3] Such nonlinear interactions can be tailored to achieve all-optical modulation, which can be based on either nonlinear loss[4−8] or frequency mixing.[9−18] For femtosecond λ = 1550 nm pulses propagating through SOI waveguides, self-phase modulation (SPM) produces pulse broadening.[5,6,19−24]

SPM in waveguides develops at sufficiently high laser intensity and mode confinement, where the optical Kerr effect creates an intensity-dependent refractive index. As a pulse propagates through a waveguide, it induces a time-varying mode index, modifying the electric field phase. This time-dependent phase appears as an instantaneous frequency of the pulse. The temporal front of the pulse experiences an increasing refractive index, yielding a red-shift, whereas the temporal back perceives a decreasing refractive index, producing a blue-shift. TPA-excited free carriers decrease the refractive index due to plasma dispersion, leading to spectral blue-shifting,[21] and impart additional absorption via FCA. Therefore, pulse broadening in SOI waveguides is generally not spectrally symmetric.

The extent to which a pulse broadens depends on its intensity, I, and the waveguide mode confinement, which are quantified by the nonlinear parameter[25]

$$\gamma = \frac{2\pi}{\lambda} \frac{\int_{-\infty}^{\infty}\int_{-\infty}^{\infty} n_2(x, y)\, I^2(x, y)\, \mathrm{d}x\, \mathrm{d}y}{\left(\int_{-\infty}^{\infty}\int_{-\infty}^{\infty} I(x, y)\, \mathrm{d}x\, \mathrm{d}y\right)^2}$$

where n_2 is the nonlinear refractive index. Nonlinear losses attenuate the pulse as it traverses the waveguide, leading to SPM saturation. The extent of SPM saturation is expressed by the nonlinear figure of merit:[26]

$$\mathrm{FOM} = \frac{n_2}{\beta_{\mathrm{TPA}}\lambda}$$

where β_{TPA} is the TPA coefficient. For Si at λ = 1550 nm, typical values[2] are β_{TPA} = 0.69 cm/GW and $n_2 = 3.2 \times 10^{-14}$ cm^2/W, producing FOM = 0.30.

Another critical consideration for SPM is chromatic dispersion.[27,28] In the case of femtosecond pulse propagation and supercontinuum generation, the nonlinear interactions and SPM-induced broadening depend on whether normal or anomalous dispersion takes place. In general, dispersion is detrimental to pulse broadening, particularly in centimeter-length waveguides. To minimize dispersion in our experiments, we consider short waveguides with L = 610 μm. Therefore, spectral pulse evolution arises predominantly from nonlinear interactions rather than linear dispersion.

Previous investigations into pulse broadening in SOI waveguides have studied the input power dependence,[5,6,19−22]

Received: January 20, 2014
Published: June 6, 2014

the influence of laser wavelength,[21] and applying SPM to nonlinear circuitry.[6] However, there have been no experimental investigations into the waveguide geometry dependence or, equivalently, the mode-profile dependence of SPM in SOI waveguides. Furthermore, there is little understanding of the interplay between mode confinement, SPM, TPA, FCA, and plasma dispersion and how these effects collectively determine power scaling of various pulse frequencies.

Here, we investigate SPM-induced spectral broadening of λ = 1550 nm femtosecond pulses in SOI waveguides with cross-sectional dimensions spanning a factor of 16. We discover unique wavelength-specific power-scaling trends that result from an exchange between SPM, TPA, FCA, and plasma dispersion. These interactions allow for wavelength-specific ultrafast nonlinear functionalities in a single SOI waveguide. Such investigations are crucial for designing ultrafast nonlinear integrated photonic devices for telecommunication wavelengths.

Figure 1a depicts the waveguide geometry and dimensions, and a top-view scanning electron micrograph (SEM) of an exemplary waveguide with length L = 610 μm, width w = 450 nm, and height h = 340 nm is shown in Figure 1b. Figure 2 displays the quasi-TM mode profile intensity distributions for waveguides with h = 340 nm (fixed) and widths w = 260, 340, 470, 540, 760, and 1000 nm. The maximum intensity, I_{max}, in each Si waveguide for peak input power, P_{peak} = 75 W, is listed in the subfigures. As w decreases, I_{max} increases due to decreasing effective waveguide mode area, A_{eff}. For the waveguides with w = 260 nm and w = 340 nm, a large fraction (54.3% for w = 260 nm, 43.8% for w = 340 nm) of the mode energy propagates outside the Si cores. However, I_{max} values within the Si cores are approximately equal (within 4%). Regardless, these modes have very distinct SPM-induced spectral broadening, indicating that the waveguide mode profile plays a key role in the SPM interaction rather than the peak intensity alone.

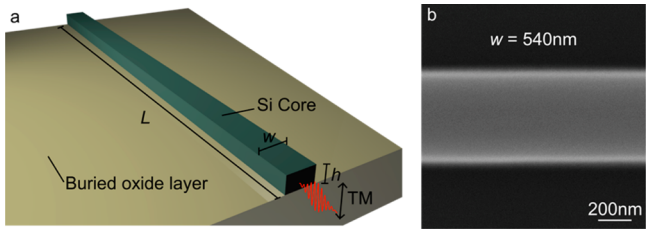

Figure 1. (a) SOI waveguide schematic. (b) Top-view SEM of w = 540 nm waveguide.

To examine this premise, we first study the effective refractive index, n_{eff}, as a function of w, for the quasi-TM mode in waveguides with h = 340 nm. As illustrated in Figure 3a, for waveguides with w > 1 μm, n_{eff} is relatively constant (~2.72). For waveguides with w < 1 μm, n_{eff} decreases with decreasing w, and for w = 260 nm, an effective refractive index of n_{eff} = 1.99 is calculated. The fraction of power propagating inside the Si waveguide core is shown as a function of w in Figure 3b, along with the nonlinear parameter, γ, which is similar to previous trends.[29] For waveguides with w > 400 nm, ~59 −68% of the λ = 1550 nm power is confined to the Si core. However, as w is decreased below w = 400 nm, the fraction of power propagating in the Si core diminishes rapidly from 0.59 to 0.34 at w = 200 nm. Clearly, the optimum width for observing nonlinear interactions in a SOI waveguide is w = 300 nm, as it offers the maximum γ (=0.59 cm^{-1} W^{-1}). Notably, changing the device layer thickness or mode polarization (i.e., 220 nm thickness, quasi-TE mode) would change only the nonlinear parameter, γ, and would not fundamentally change the nonlinear interactions.

Femtosecond pulses with τ_p = 84 fs duration, 90 MHz repetition rate, and λ = 1550 nm center wavelength were used to investigate nonlinear optical interactions in waveguides. Although a high numerical aperture microscope objective enables tight focusing and high coupling efficiency, it reduces polarization purity, and additional waveguide modes are excited, introducing measurement inaccuracies. Therefore, more gradual focusing is sometimes beneficial, at the expense of lower coupling efficiency. An NA = 0.65 objective was found to offer a good trade-off in this regard. The microscope objective was used to focus pulses on the waveguide input facets, and a lensed optical fiber was used to out-couple

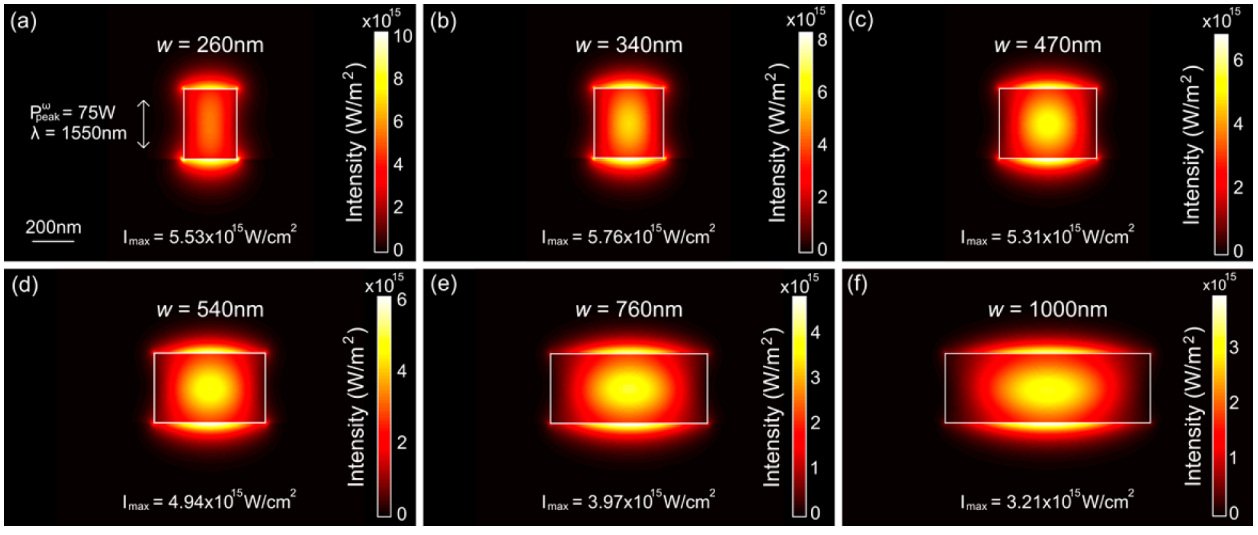

Figure 2. Mode profile intensity distributions for P_{peak} = 75 W, h = 340 nm, and w = (a) 260 nm, (b) 340 nm, (c) 470 nm, (d) 540 nm, (e) 760 nm, and (f) 1000 nm.

dx.doi.org/10.1021/ph500022f | ACS Photonics 2014, 1, 576−581

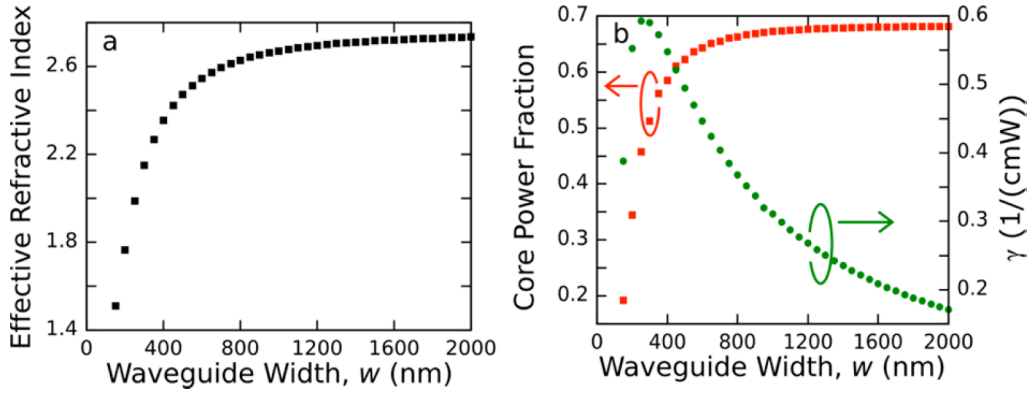

Figure 3. (a) Effective refractive index as a function of w and h = 340 nm (fixed). (b) Fraction of mode power confined to the Si core (red squares) and the nonlinear parameter, γ (green circles), as a function of w.

transmitted pulses. The laser pulse polarization was oriented to excite the quasi-TM waveguide mode.

A critical parameter for understanding nonlinear interactions in SOI waveguides is the free-carrier recombination time, τ_r. Ultrafast pump−probe measurements were performed on the waveguides, where the nonlinear loss introduced by a strong pump pulse was mapped onto the transmission of a weaker probe pulse.[30] From these measurements (outlined in the Supporting Information), τ_r = 265 ps was extracted, which is shorter than the period between pulses (T = 11.1 ns). Therefore, free carriers excited by a particular pulse recombine before the subsequent pulse arrives and any free-carrier dispersion imparted on a pulse must arise from free carriers excited by that same pulse. This free-carrier lifetime is comparable to previous lifetimes that have been measured in SOI waveguides with similar dimensions.[2,31] Since h = 340 nm was unchanged, no systematic relationship between τ_r and w was observed.

Typical transmitted spectra from a w = 340 nm waveguide are shown on a logarithmic y-axis in Figure 4. The spectrum

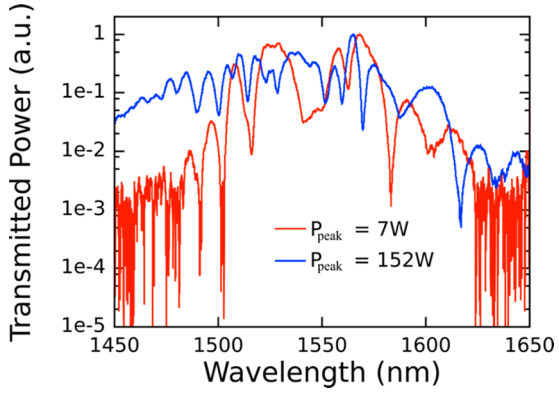

Figure 4. Transmitted pulse spectra for a waveguide with w = 340 nm and L = 615 μm for P_{peak} = 7 W (red) and P_{peak} = 152 W (blue).

obtained at P_{peak} = 7 W (red) is taken below the threshold for nonlinear interaction and represents linear pulse transmission through the waveguide. Virtually no power is observed for λ < 1480 nm or λ > 1625 nm. The spectrum taken at P_{peak} = 152 W (blue) is broadened via SPM, indicating strong nonlinear interactions within the Si core. The power of spectral components in the range 1450 nm ≤ λ ≤ 1480 nm increases 225-fold, whereas components in the range 1625 nm ≤ λ ≤ 1650 nm are enhanced 15-fold. Interestingly, distinct spectral components exhibit decreasing power with increasing P_{peak}. This suggests more complex interactions than SPM alone and is evidence of interplay between SPM, TPA, FCA, and plasma dispersion.

To investigate this interplay, it is insightful to examine the evolution of various spectral components for increasing P_{peak}. The surface plot in Figure 5a depicts the transmitted pulse spectrum as a function of P_{peak} for the w = 340 nm waveguide. Significant spectral reshaping and broadening is evident as P_{peak} is increased above P_{peak} = 20 W. The most noticeable transformations are the appearance of spectral components in the range 1535 nm ≤ λ ≤ 1550 nm and multiple sidebands at λ ≤ 1480 nm and λ ≥ 1590 nm. Figure 5b displays the entire integrated transmitted spectrum for each P_{peak}. Notably, for P_{peak} ≤ 20 W, the trend is approximately linear, but nonlinear loss (i.e., TPA and FCA) gradually saturates the transmitted power, and for P_{peak} ≥ 110 W, subsequent increases in P_{peak} yield negligible increases in transmitted power.

While the power dependence in Figure 5b is well known, it does not apply to individual spectral pulse components, as strong spectral reshaping takes place and growth or saturation of specific wavelengths may not exhibit the same behavior. It is more insightful to investigate power scaling for various wavelength regions of the pulse. This is particularly important for ultrafast all-optical wavelength-dependent modulation devices. To illustrate this property, several spectral slices depicting different power-scaling trends are shown in Figure 5c−f. Figure 5c represents the power transmitted in the range 1517 nm ≤ λ ≤ 1519 nm, a region where little laser power is delivered. For P_{peak} < 50 W, virtually no power is transmitted in this region, as no SPM has occurred to generate wavelengths here. For P_{peak} > 50 W, a substantial TPA-excited free-carrier population ($N \approx 10^{19}$−10^{20} cm^{-3}) gives rise to plasma dispersion and spectral blue-shifting (see Figure 5a). In this case, an adjacent spectral peak blue-shifts into this spectral range, yielding superlinear growth.

Figure 5d depicts the power scaling in the range 1535.7 nm ≤ λ ≤ 1542 nm. Similar to the power scaling integrated over the entire pulse spectrum, the relation is linear for P_{peak} ≤ 20 W. Further increases in power produce a slight increase in the growth trend due to SPM, which continues until P_{peak} = 90 W. Subsequent increases in P_{peak} produce saturation and even negative differential transmission due to TPA and FCA.

A far different power-scaling trend for 1552.6 nm ≤ λ ≤ 1559.6 nm is shown in Figure 5e, where again there is linear

dx.doi.org/10.1021/ph500022f | ACS Photonics 2014, 1, 576−581

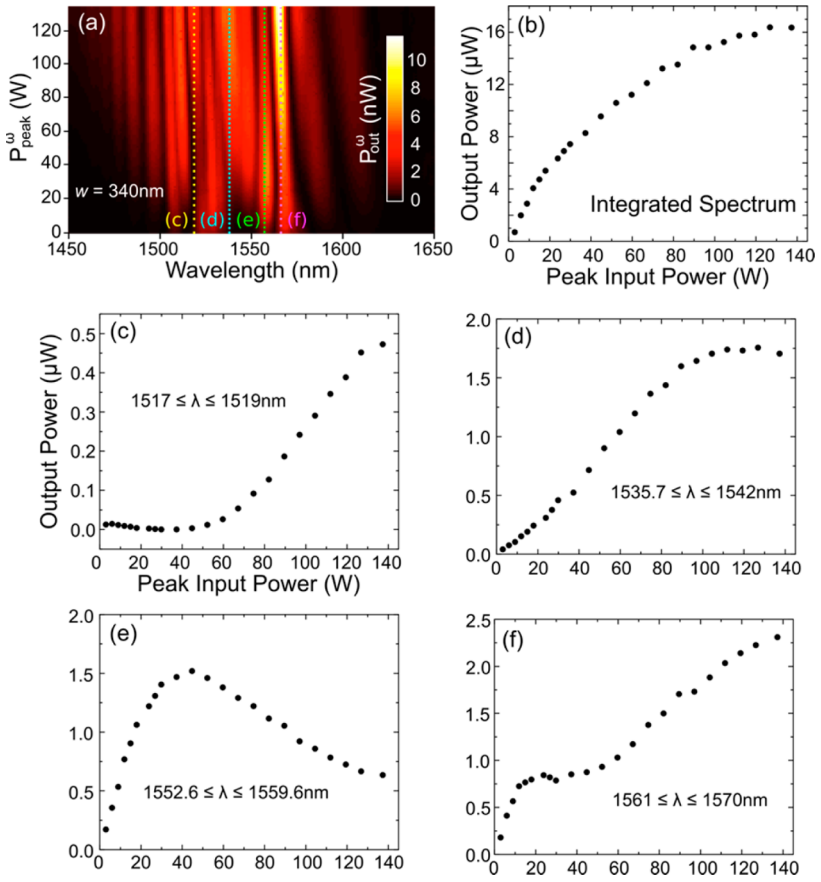

Figure 5. (a) Surface depicting the transmitted pulse spectrum versus P_{peak} for a w = 340 nm waveguide. (b) Total transmitted pulse power versus P_{peak} depicting TPA- and FCA-induced transmission saturation. Transmitted spectral power is also calculated for the ranges (c) 1517 nm ≤ λ ≤ 1519 nm; (d) 1535.7 nm ≤ λ ≤ 1542 nm; (e) 1552.6 nm ≤ λ ≤ 1559.6 nm; and (f) 1561 nm ≤ λ ≤ 1570 nm.

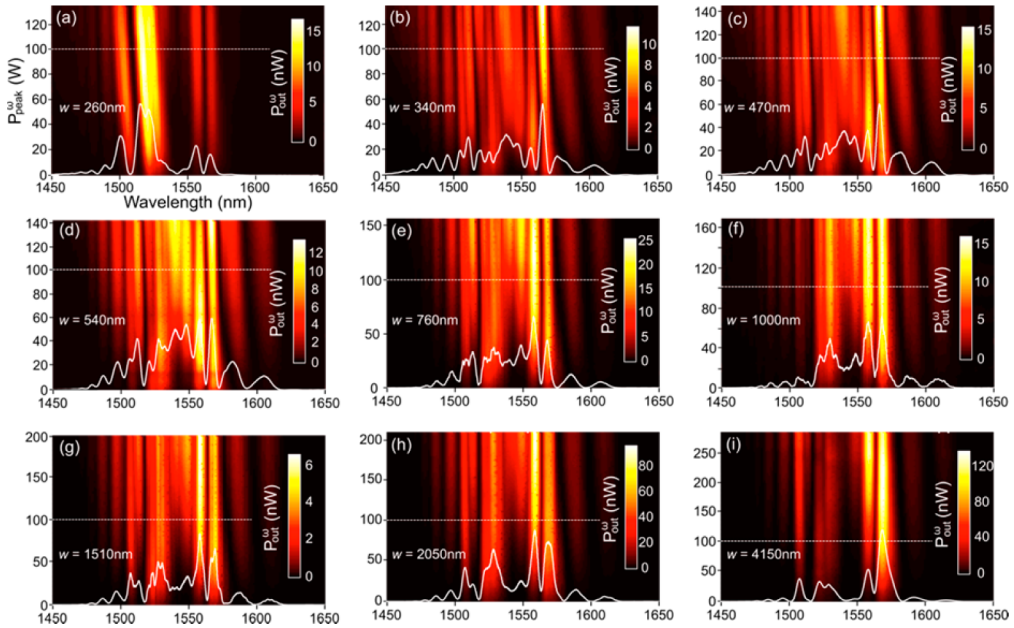

Figure 6. Surfaces depicting the transmitted pulse spectrum versus P_{peak} for waveguides with w = (a) 260 nm, (b) 340 nm, (c) 470 nm, (d) 540 nm, (e) 760 nm, (f) 1000 nm, (g) 1510 nm, (h) 2050 nm, and (i) 4150 nm. Sections of the transmitted spectrum at P_{peak} = 100 W are plotted in white.

growth for P_{peak} ≤ 20 W. However, this spectral region exhibits strong saturation at much lower P_{peak} = 44.8 W and large negative differential transmission due to SPM, TPA, and FCA collectively. Notably, the power transmitted in this spectral range at P_{peak} = 137 W is less than half the maximum transmitted power (P_{peak} = 44.8 W).

Figure 5f shows the power scaling for 1561 nm ≤ λ ≤ 1570 nm. Here, evidence of transmission saturation occurs at much

dx.doi.org/10.1021/ph500022f | ACS Photonics 2014, 1, 576−581

lower powers (12 W ≤ P_{peak} ≤ 40 W), and further increases in P_{peak} increase the transmitted power without noticeable saturation. For P_{peak} ≥ 40 W, SPM, TPA, and FCA do not influence the transmitted power as significantly as the spectral ranges of Figure 5d,e. Indeed, the distinct wavelength-dependent power-scaling trends allow for multiple functionalities in a single waveguide.

These wavelength-dependent power-scaling trends are not unique to the w = 340 nm waveguide. Each waveguide width exhibited essentially the same trends for these spectral windows. However, due to different mode confinement, I_{max} inside the Si cores, and n_{eff}, certain spectral features occur at different peak powers and have different amplitudes relative to adjacent features. In particular, the waveguides with w = 340, 470, and 540 nm scaled with virtually identical trends, whereas the w = 260 nm waveguide deviated the most (discussed subsequently).

Surfaces depicting the transmitted spectrum as a function of P_{peak} for the waveguides are presented in Figure 6. The strongest SPM is observed for w = 340, 470, 540, and 760 nm. In these waveguides, strong mode confinement yields a high nonlinear parameter, γ. Interestingly, no distinct SPM is observed for w = 260 nm. Instead, the spectral peak is blue-shifted from λ = 1522.3 nm to λ = 1514.9 nm, evidencing a large TPA-induced free-carrier population ($N \approx 10^{19}$cm^{-3}); TPA and FCA rapidly reduce P_{peak} in the waveguide, before significant broadening accumulates. Furthermore, wavelength-dependent propagation loss is observed, which arises from high mode delocalization. Delocalization increases for longer pulse wavelengths, which interact more strongly with the waveguide sidewalls and experience greater attenuation than shorter pulse wavelengths.

The larger waveguides depicted in Figures 6f–i (i.e., 1000 nm ≤ w ≤ 4150 nm) have a significantly lower γ (≤0.31 cm^{-1} W^{-1}) and operate with multiple modes. Therefore, as w is increased, SPM-induced pulse broadening becomes less pronounced, particularly for 1535 nm ≤ λ ≤ 1550 nm, λ ≤ 1480 nm, and λ ≥ 1580 nm. For the largest waveguide (w = 4150 nm), SPM-induced spectral features are very weak relative to the main pulse components.

In summary, we have investigated several nonlinear optical effects in SOI waveguides. The large $\chi^{(3)}$ coefficient of Si enables observation of strong SPM in a short waveguide with L = 610 μm. The strongest broadening is observed in waveguides with 340 nm ≤ w ≤ 760 nm. For a smaller waveguide with w = 260 nm, strong TPA and FCA saturate the SPM. For waveguides with w > 760 nm, a combination of lower mode confinement and multimode operation give rise to less-pronounced broadening. Interesting power-scaling trends are observed in several spectral bands, which can be exploited for ultrafast wavelength-dependent switching and other functionalities. This will allow for unique wavelength-dependent nonlinear functionalities to be performed in a single structure, increasing the functionality of SOI waveguides for integrated optical circuitry. These results may be straightforwardly applied to the common SOI thickness of 220 nm and quasi-TE modes.

■ ASSOCIATED CONTENT

Supporting Information

Information related to the measurement of the free-carrier recovery time and the waveguide fabrication process is available free of charge via the Internet at http://pubs.acs.org.

■ AUTHOR INFORMATION

Corresponding Author

*E-mail: elezzabi@ece.ualberta.ca.

Present Address

†Max-Planck-Institute of Quantum Optics, Hans-Kopfermann-Str. 1, D85748 Garching, Germany

Author Contributions

The manuscript was written through contributions of all authors. All authors have given approval to the final version of the manuscript.

Notes

The authors declare no competing financial interest.

■ ACKNOWLEDGMENTS

This work was supported by the Natural Sciences and Engineering Research Council of Canada and Alberta Innovates.

■ REFERENCES

(1) Dekker, R.; Usechak, N.; Först, M.; Driessen, A. Ultrafast nonlinear all-optical processes in silicon-on-insulator waveguides. *J. Phys. D: Appl. Phys.* **2007**, *40*, R249–R271.

(2) Motamedi, A. R.; Nejadmalayeri, A. H.; Khilo, A.; Kärtner, F.; Ippen, E. P. Ultrafast nonlinear optical studies of silicon nanowaveguides. *Opt. Express* **2012**, *20*, 4085–4101.

(3) Sederberg, S.; Elezzabi, A. Y. Nonlinear response of an ultracompact waveguide Fabry-Pérot resonator. *Appl. Phys. Lett.* **2013**, *102*, 011133.

(4) Tsang, H. K.; Wong, C. S.; Liang, T. K.; Day, I. E.; Roberts, S. W.; Harping, A.; Drake, J.; Asghari, M. Optical dispersion, two-photon absorption and self-phase modulation in silicon waveguides at 1.5μm wavelength. *Appl. Phys. Lett.* **2002**, *80*, 416–818.

(5) Rieger, G. W.; Virk, K. S.; Young, J. F. Nonlinear propagation of ultrafast 1.5μm pulses in high-index-contrast silicon-on-insulator waveguides. *Appl. Phys. Lett.* **2004**, *84*, 900–903.

(6) Cowan, A. R.; Rieger, G. W.; Young, J. F. Nonlinear transmission of 1.5μm pulses through single-mode silicon-on-insulator waveguide structures. *Opt. Express* **2004**, *12*, 1611–1621.

(7) Moss, D. J.; Fu, L.; Littler, I.; Eggleton, B. J. Ultrafast all-optical modulation via two-photon absorption in silicon-on-insulator waveguides. *Electron. Lett.* **2005**, *41*, 320–321.

(8) Liang, T.; Nunes, L. R.; Sakamoto, T.; Sasagawa, K.; Kawanishi, T.; Tsuchiya, M.; Priem, G. R. A.; van Thourhout, D.; Dumon, P.; Baets, R.; Tsang, H. K. Ultrafast all-optical switching by cross-absorption modulation in silicon wire waveguides. *Opt. Express* **2005**, *13*, 7298–7303.

(9) Espinola, R. L.; Dadap, J. I.; Osgood, R. M.; McNab, S. J.; Vlasov, Y. A. C-Band wavelength conversion in silicon photonic wire waveguides. *Opt. Express* **2005**, *13*, 4341–4349.

(10) Fukuda, H.; Yamada, K.; Shoji, T.; Takahashi, M.; Tsuchizawa, T.; Watanabe, T.; Takahashi, J.; Itabashi, S. Four-wave mixing in silicon wire waveguides. *Opt. Express* **2005**, *13*, 4629–4637.

(11) Foster, M. A.; Turner, A. C.; Sharping, J. E.; Schmidt, B. S.; Lipson, M.; Gaeta, A. L. Broad-band optical parametric gain on a silicon photonic chip. *Nature* **2006**, *441*, 960–963.

(12) Lin, Q.; Zhang, J.; Fauchet, P. M.; Agrawal, G. P. Ultrabroadband parametric generation and wavelength conversion in silicon waveguides. *Opt. Express* **2006**, *14*, 4786–4799.

(13) Foster, M. A.; Turner, A. C.; Salem, R.; Lipson, M.; Gaeta, A. L. Broad-band continuous-wave parametric wavelength conversion in silicon nanowaveguides. *Opt. Express* **2007**, *15*, 12949–12958.

(14) Salem, R.; Foster, M. A.; Turner, A. C.; Geraghty, D. F.; Lipson, M.; Gaeta, A. L. Signal regeneration using low-power four-wave mixing on silicon chip. *Nat. Photonics* **2008**, *2*, 35–38.

(15) Dekker, R.; Driessen, A.; Wahlbrink, T.; Moormann, C.; Niehusmann, J.; Först, M. Ultrafast Kerr-induced all-optical wave-

length conversion in silicon waveguides using 1.55μm femtosecond pulses. *Opt. Express* **2006**, *14*, 8336−8346.
(16) Zlatanovic, S.; Park, J. S.; Moro, S.; Boggio, J. M. C.; Divliansky, I. B.; Alic, N.; Mookherjea, S.; Radic, S. Mid-infrared wavelength conversion in silicon waveguides using ultracompact telecom-band-derived pump source. *Nat. Photonics* **2010**, *4*, 561−564.
(17) Kuyken, B.; Liu, X.; Osgood, R. M., Jr.; Vlasov, Y.; Roelkens, G.; Baets, R.; Green, W. M. J. Frequency-conversion of mid-infrared optical signals into the telecom band using nonlinear silicon nanophotonic wires. *Optical Fiber Communication Conference* 2011, OThU4.
(18) Lau, R. K. W.; Menard, M.; Okawachi, Y.; Foster, M. A.; Turner-Foster, A. C.; Salem, R.; Lipson, M.; Gaeta, A. L. Continuous-wave mid-infrared frequency conversion in silicon nanowaveguides. *Opt. Lett.* **2011**, *36*, 1263−1265.
(19) Boyraz, Ö.; Koonath, P.; Raghunathan, V.; Jalali, B. All optical switching and continuum generation in silicon waveguides. *Opt. Express* **2004**, *12*, 4094−4102.
(20) Boyraz, Ö.; Indukuri, T.; Jalali, B. Self-phase-modulation induced spectral broadening in silicon waveguides. *Opt. Express* **2004**, *12*, 829−834.
(21) Dulkeith, E.; Vlasov, Y. A.; Chen, X.; Panoiu, N. X.; Osgood, R. M. Self-phase-modulation in submicron silicon-on-insulator photonic wires. *Opt. Express* **2006**, *14*, 5524−5534.
(22) Hsieh, I.-W.; Chen, X.; Dadap, J. I.; Panoiu, N. C.; Osgood, R. M.; McNab, S. J.; Vlasov, Y. A. Ultrafast-pulse self-phase modulation and third-order dispersion in Si photonic wire-waveguides. *Opt. Express* **2006**, *14*, 12380−12387.
(23) Kuyken, B.; Liu, X.; Osgood, R. M., Jr.; Baets, R.; Roelkens, G.; Green, W. M. J. Mid-infrared to telecom-band supercontinuum generation in highly nonlinear silicon-on-insulator waveguides. *Opt. Express* **2011**, *19*, 20172−20181.
(24) Hsieh, I.-W.; Chen, X.; Liu, X.; Dadap, J. I.; Panoiu, N. C.; Chou, C.-Y.; Xia, F.; Green, W. M.; Vlasov, Y. A.; Osgood, R. M., Jr. Supercontinuum generation in silicon photonic wires. *Opt. Express* **2007**, *15*, 15242−15249.
(25) Agrawal, G. P. *Nonlinear Fiber Optics*; Academic Press: San Diego, 2013; pp 38 − 39.
(26) Koos, C.; Jacome, L.; Poulton, C.; Leuthold, J.; Freude, W. Nonlinear silicon-on-insulator waveguides for all-optical signal processing. *Opt. Express* **2007**, *15*, 5976−5990.
(27) Lin, L.; Lin, Q.; Agrawal, G. P. Soliton fission and supercontinuum generation in silicon waveguides. *Opt. Lett.* **2007**, *32*, 391−393.
(28) Zhang, L.; Lin, Q.; Yue, Y.; Yan, Y.; Beausoleil, R. G.; Willner, A. E. Silicon waveguide with four zero-dispersion wavelengths and its application in on-chip supercontinuum generation. *Opt. Express* **2012**, *20*, 685−1690.
(29) Foster, M. A.; Moll, K. D.; Gaeta, A. L. Optimal waveguide dimensions for nonlinear interactions. *Opt. Express* **2004**, *12*, 2880−2887.
(30) Boggess, T. F.; White, J. O.; Valley, G. C. Two-photon absorption and anisotropic transient energy transfer in $BaTiO_3$ with 1-psec excitation. *J. Opt. Soc. Am. B* **1990**, *7*, 2255−2258.
(31) Almeida, V. R.; Barrios, C. A.; Panepucci, R. R.; Lipson, M.; Foster, M. A.; Ouzounov, D. G.; Gaeta, A. L. All-optical switching on a silicon chip. *Opt. Lett.* **2004**, *29*, 2867−2869.